

Bessel beam through a dielectric slab at oblique incidence: the case of total reflection

D. Mugnai*

*“Nello Carrara” Institute of Applied Physics - CNR [†]
50127 Firenze, Italy*

August 29, 2018

Abstract

The oblique incidence of a Bessel beam on a dielectric slab with refractive index n_1 surrounded by a medium of a refractive index $n > n_1$ may be studied simply by expanding the Bessel beam into a set of plane waves forming the same angle θ_0 with the axis of the beam. In the present paper we examine a Bessel beam that impinges at oblique incidence onto a layer in such a way that each plane-wave component impinges with an angle larger than the critical angle.

The propagation of a Bessel beam, or Bessel wave[1], represents an interesting topic both for its implication in relation to superluminal motion[2, 3], and for its spatial localization, which makes it a good candidate for all practical applications where a localized field is required[4, 5].

The propagation of a Bessel beam through a dielectric slab, for normal incidence and in the presence of total reflection, has already been analyzed by Shaarawi and Besieris[6] and Mugnai[7]. Furthermore, propagation in a layered medium for normal and oblique incidences, in the absence of total reflection, has also been studied[8].

The aim of the present work is to analyze a Bessel beam impinging onto a plane slab at oblique incidence, in the case in which all the waves forming the beam are in total reflection. The main interest of this kind of analysis is to investigate if the beam propagates by maintaining its characteristic of localized wave also in the case of oblique incidence.

Let us consider a simple system formed by two half-spaces that are filled with a homogeneous and non-dispersive medium of refractive index n , and separated

*d.mugnai@ifac.cnr.it

[†]Former: “Nello Carrara” Electromagnetic Waves Research Institute

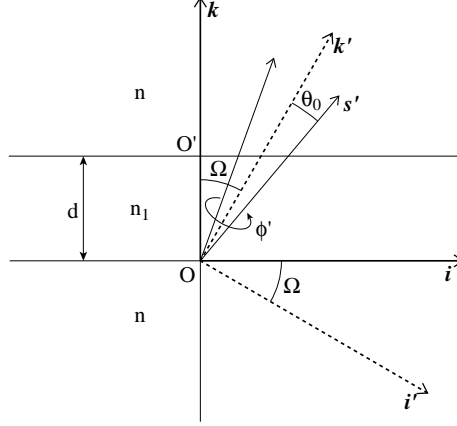


Figure 1: Slab, of finite thickness d , of a medium with refractive index n_1 , surrounded on both sides by a different medium with refractive index $n > n_1$. The reference system S , of unit vectors \mathbf{i} , \mathbf{j} , \mathbf{k} , is shown together with the system S' , rotated of an angle Ω with respect to S . The vector \mathbf{s}' represents the direction of propagation of a single plane wave. The contribution of all the plane waves, making the same angle θ_0 with the z' axis, generates a Bessel beam characterized by the axicon angle θ_0 and whose axis of symmetry is coincident with z' . The angle ϕ' is the azimuthal angle in the plane $x'y'$.

by a gap, of thickness d , filled with a medium of refractive index $n_1 < n$ (see Fig. 1). We refer the space to a system, S , of Cartesian coordinates x, y, z (unit vector $\mathbf{i}, \mathbf{j}, \mathbf{k}$), with the xy plane coinciding with the input boundary of the layer, and the \mathbf{k} axis normal to the boundaries. Let us consider a monochromatic plane wave, impinging onto the layer, which can be written as[9]

$$u^i = A^i \exp[ik_0 n(\alpha x + \beta y + \gamma z)] \exp(-i\omega t), \quad (1)$$

where A_i is the amplitude at the origin O , $k_0 = \omega/c$ (ω is the angular frequency of the wave), and α, β, γ are the directions cosines. Without loss of generality, from here on, we shall omit the temporal factor and we assume $A^i = 1$.

In Refs. [10] and [11] it has been shown that, within the same reference system, the transmitted u^t and the reflected u^r plane waves can be expressed as

$$u^t = T \exp[ik_0 n(\alpha x + \beta y + \gamma(z - d))] \quad (2)$$

$$u^r = R \exp[ik_0 n(\alpha x + \beta y - \gamma z)], \quad (3)$$

where T and R are the given by

$$T = \frac{4inn_1\gamma\Gamma}{e_2(n\gamma + in_1\Gamma)^2 - e_1(n\gamma - in_1\Gamma)^2} \quad (4)$$

$$R = \frac{T}{2n_1\Gamma} [n_1\Gamma(e_1 + e_2) + in\gamma(e_1 - e_2)] - 1, \quad (5)$$

with

$$\begin{aligned} e_1 &= \exp(-k_0n_1\Gamma d), \\ e_2 &= \exp(k_0n_1\Gamma d), \\ \Gamma^2 &= \frac{1}{n_1^2} (n^2 - n_1^2 - n^2\gamma^2). \end{aligned} \quad (6)$$

The quantity T represents the complex amplitude of the transmitted wave at O' , and R that of the reflected wave at O . Note that both T and R depend only on γ and not on α and β .

The above expressions hold when the angle of incidence i onto the layer is larger than the critical angle i_0 : this implies that $\sin i > n_1/n$, or, since $\cos i = \gamma$, that $\gamma^2 < 1 - (n_1^2/n^2)$ and Γ is real.

Let us now consider a set of plane waves, of the type given in Eq. (1), having the same complex amplitude at O and whose directions of propagation form the same angle θ_0 with the axis \mathbf{k} .

As usual, we can write the direction cosines as

$$\begin{aligned} \alpha &= \sin \theta_0 \cos \phi \\ \beta &= \sin \theta_0 \sin \phi \\ \gamma &= \cos \theta_0, \end{aligned} \quad (7)$$

where ϕ is the azimuthal angle in xy plane. The superposition of all these waves creates a Bessel beam, U_B , whose axis, \mathbf{k}_b , is normal to the boundaries of the layer ($\mathbf{k}_b \equiv \mathbf{k}$) [7],

$$U_B^i = J_0(k_0n\rho \sin \theta_0) \exp(ik_0n \cos \theta_0 z), \quad (8)$$

where ρ represents the cylindrical coordinate in the plane normal to the axis of the beam ($\rho^2 = x^2 + y^2$). The Bessel beam is, therefore, expressed as an expansion in plane waves, the directions of propagation of which cover a conical surface of half angle θ_0 (axicon angle). Thus, since each plane wave impinges onto the layer with the same incidence angle θ_0 , the refraction angle θ' ($\sin \theta' = n \sin \theta_0 / n_1$) will also be the same for all the waves. Consequently, the transmitted plane waves turn out to have the same complex amplitude at O' , and the transmitted beam is found to be [7, 6]

$$U_B^t = T J_0(k_0n\rho \sin \theta_0) \exp[ik_0n(z - d) \cos \theta_0]. \quad (9)$$

Analogously, the reflected plane waves turn out to have the same complex amplitude at O , and their integration over ϕ constitutes the reflected Bessel beam:

$$U_B^r = RJ_0(k_0 n \rho \sin \theta_0) \exp(-ik_0 n z \cos \theta_0) . \quad (10)$$

Let us consider now the case of oblique incidence, that is when $\mathbf{k}_b = \mathbf{k}' \neq \mathbf{k}$ [8]. In this case, it is expedient to introduce another reference system, S' , whose axis \mathbf{k}' is rotated in the xz -plane of a given angle Ω with respect to \mathbf{k} (see Fig. 1). The Cartesian axes $\mathbf{i}', \mathbf{j}', \mathbf{k}'$ of S' are related to $\mathbf{i}, \mathbf{j}, \mathbf{k}$ by

$$\begin{aligned} \mathbf{i}' &= \gamma_k \mathbf{i} - \alpha_k \mathbf{k} \\ \mathbf{j}' &= \mathbf{j} \\ \mathbf{k}' &= \alpha_k \mathbf{i} + \gamma_k \mathbf{k} , \end{aligned} \quad (11)$$

where $\alpha_k = \sin \Omega$, $\gamma_k = \cos \Omega$.

The incident Bessel beam now consists of a set of plane waves, all forming the same angle θ_0 with \mathbf{k}' . This implies that the plane-wave component impinges onto the first interface of the slab with different angles of incidence. It turns out that the incidence angle varies from $\theta_0 - \Omega$ to $\theta_0 + \Omega$ when ϕ ranges from 0 to 2π .

The generic incidence vector \mathbf{s}' can be written as

$$\mathbf{s}' = \alpha' \mathbf{i}' + \beta' \mathbf{j}' + \gamma' \mathbf{k}' \quad (12)$$

with

$$\begin{aligned} \alpha' &= \sin \theta_0 \cos \phi' \\ \beta' &= \sin \theta_0 \sin \phi' \\ \gamma' &= \cos \theta_0 , \end{aligned} \quad (13)$$

where ϕ' is the azimuthal angle in plane $x'y'$. Thus, the incidence field due to a generic wave at a given point P of the space is given by

$$u_{ob}^i = A^i \exp[ik_0 n \mathbf{s}' \cdot \vec{OP}] , \quad (14)$$

and, since $\vec{OP} = x\mathbf{i} + y\mathbf{j} + z\mathbf{k}$ (or $= x'\mathbf{i}' + y'\mathbf{j}' + z'\mathbf{k}'$), by considering Eqs. (11)-(13), we obtain

$$u_{ob}^i = \exp\{ik_0 n [\alpha_{\phi'} x + \beta_{\phi'} y + \gamma_{\phi'} z]\} , \quad (15)$$

where

$$\begin{aligned} \alpha_{\phi'} &= \gamma_k \sin \theta_0 \cos \phi' + \alpha_k \cos \theta_0 \\ \beta_{\phi'} &= \sin \theta_0 \sin \phi' \\ \gamma_{\phi'} &= \gamma_k \cos \theta_0 - \alpha_k \sin \theta_0 \cos \phi' . \end{aligned} \quad (16)$$

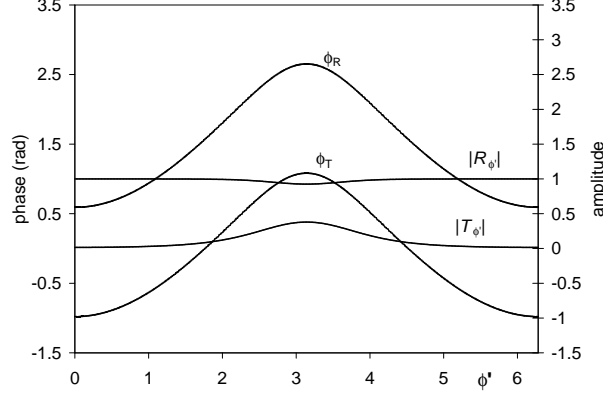


Figure 2: Phases and amplitudes of the reflection, R_{ob} , and transmission, T_{ob} , coefficients, as a function of the azimuthal angle ϕ' . Parameter values are: $\omega = 60$ rad/s, $n = 1.5$, $n_1 = 1$, $\Omega \simeq 18^\circ$ ($\alpha_k = 0.3$), $\theta_0 = 60^\circ$, $d = 2$ cm. For this value of θ_0 , $\Omega = 18^\circ$ represents the limit angle of rotation: for higher values of Ω , not all the waves forming the beam are in total reflection.

For the reflected u_{ob}^r and transmitted u_{ob}^t fields, we have

$$u_{ob}^r = R_{ob} \exp \{ik_0 n [\alpha_{\phi'} x + \beta_{\phi'} y - \gamma_{\phi'} z]\} \quad (17)$$

$$u_{ob}^t = T_{ob} \exp \{ik_0 n [\alpha_{\phi'} x + \beta_{\phi'} y + \gamma_{\phi'} (z - d)]\} . \quad (18)$$

The reflection R_{ob} and transmission T_{ob} coefficients can be still expressed by means of Eqs. (4) and (5), with γ replaced by $\gamma_{\phi'}$ everywhere. Consequently, T_{ob} and R_{ob} depend on ϕ' as well:

$$T_{ob} = \frac{4inn_1\gamma_{\phi'}\Gamma_{\phi'}}{e_{2\phi'}[n\gamma_{\phi'} + in_1\Gamma_{\phi'}]^2 - e_{1\phi'}[n\gamma_{\phi'} - in_1\Gamma_{\phi'}]^2} = |T_{\phi'}| \exp(i\phi_T) \quad (19)$$

$$R_{ob} = \frac{T_{\phi'}}{2n_1\Gamma_{\phi'}} \left[n_1\Gamma_{\phi'} (e_{1\phi'} + e_{2\phi'}) + in\gamma_{\phi'} (e_{1\phi'} - e_{2\phi'}) \right] - 1 = |R_{\phi'}| \exp(i\phi_R) \quad (20)$$

where

$$\Gamma_{\phi'} = \frac{1}{n_1} \sqrt{n^2(1 - \gamma_{\phi'}^2) - n_1^2}, \quad e_{1\phi'} = \exp(-k_0 n_1 \Gamma_{\phi'} d), \quad e_{2\phi'} = 1/e_{1\phi'}. \quad (21)$$

The amplitudes $|T_{\phi'}|$ and $|R_{\phi'}|$ and phases ϕ_T and ϕ_R , of T_{ob} and R_{ob} , respectively, are shown in Fig. 2 as a function of ϕ' , for $\theta_0 = 60^\circ$, $n_1 = 1$, $n = 1.5$ and $\Omega \simeq 18^\circ$ ($\alpha_k = 0.3$). With this choice of parameter values, all the waves forming the beam are in total reflection since the incidence angle of each wave is larger than the critical angle $i_0 = \sin^{-1}(1/n) = 41.8^\circ$. For $\theta_0 = 60^\circ$, the

value of $\Omega \simeq 18^\circ$ represents the maximum angle possible in order to have total reflection at the first interface.

In order to find the reflected and transmitted beams, we have to integrate Eqs. (17) and (18) over ϕ' , between 0 and 2π . In Figs. 3 and 4, we show the results of the numerical integration for both the reflected and transmitted fields as a function of the x coordinate, for $\theta_0 = 60^\circ$ and for normal ($\Omega = 0$) and oblique incidences ($\Omega \simeq 6^\circ, 11^\circ, 18^\circ$, $\alpha_k = 0.1, 0.2, 0.3$, respectively). We note that, for $\Omega \neq 0$, the transmitted field is still characterized by a main maximum and secondary maxima and minima, but suffers deformation with respect to the incident field and tends to lose its localization[12].

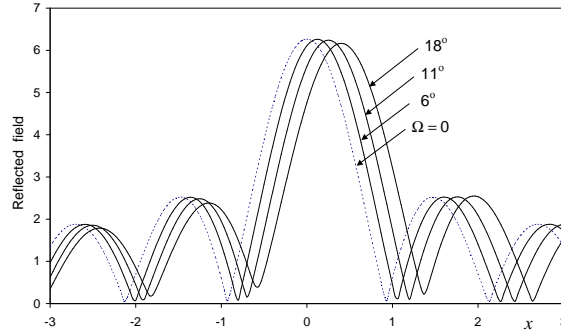


Figure 3: Reflected field as a function of the x coordinate, for normal, $\Omega = 0$ (dashed line), and oblique incidences, $\Omega \simeq 6^\circ, 11^\circ, 18^\circ$ ($\alpha_k = 0.1, 0.2, 0.3$, respectively). The reflected field is derived, for $y = 0$ and $z = 0$, by numerical integration of Eq. (17) over ϕ' , between 0 and 2π . Other parameter values are as in Fig. 2. The displacement of the field profile, with respect to the normal incidence, evidences the Goos-Hänchen effect.

Looking at Figs. 3 and 4, we note that, for the same value of Ω , the reflected field suffers less deformation with respect to the transmitted one.

The deformation of the emerging Bessel beam (Fig. 4), with respect to the incident one, can be followed by analyzing the field inside the slab (optical tunneling region). To this end, let us start again with a single plane wave. We recall that, in the absence of the second half-space ($d = \infty$), the propagation after the first surface is due to evanescent waves which propagate parallel to the slab. The presence of the second boundary at $z = d$ originates anti-evanescent (or regressive) waves, and the superposition of the two waves, as is well-known, makes the Poynting vector different from zero also in the direction perpendicular to the slab.

The progressive u^+ and regressive u^- waves within the slab can be written

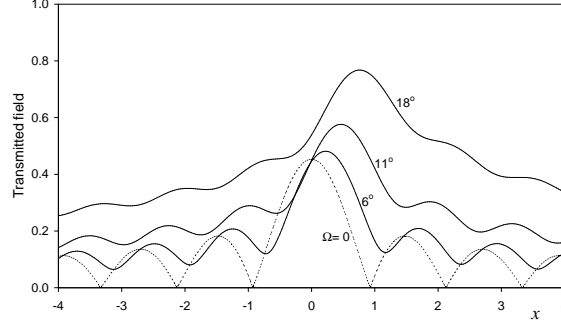


Figure 4: Transmitted field, as a function of the x coordinate, obtained by numerical integration of Eq. (18) over ϕ' , at $y = 0$ and $z = d + 1$. Other parameter values are as in Fig. 3.

as

$$u_{ob}^+ = p_{\phi'} \exp\{ik_0[n(\alpha_{\phi'}x + \beta_{\phi'}y) + in_1\Gamma_{\phi'}z]\} \quad (22)$$

$$u_{ob}^- = r_{\phi'} \exp\{ik_0[n(\alpha_{\phi'}x + \beta_{\phi'}y) - in_1\Gamma_{\phi'}z]\}. \quad (23)$$

with

$$\begin{aligned} p_{\phi'} &= \frac{e_{2\phi'}}{2n_1\Gamma_{\phi'}}(n_1\Gamma_{\phi'} - in\gamma_{\phi'})T_{\phi'} \\ r_{\phi'} &= \frac{e_{1\phi'}}{2n_1\Gamma_{\phi'}}(n_1\Gamma_{\phi'} + in\gamma_{\phi'})T_{\phi'}. \end{aligned} \quad (24)$$

Equations (24) were obtained from the continuity conditions for the tangential component of both the electric and magnetic fields across the two boundaries, at $z = 0$ and $z = d$ [10].

The field u_{tot}^g inside the gap is given by the superposition of progressive u^+ and regressive u^- waves of Eqs. (22) and (23), and can be expressed as

$$u_{tot}^g = \exp[i(k_0n(\alpha_{\phi'}x + \beta_{\phi'}y))] |T_{\phi'}| e^{i\phi_T} \frac{1}{n_1\Gamma_{\phi'}} \left[|A^g| e^{i\eta(z)} \right] \quad (25)$$

where $|T_{\phi'}|$ and ϕ_T can be derived from Eq. (19). The quantities $|A^g|$ and $\eta(z)$, in Eq. (25), are given by

$$\begin{aligned} |A^g| &= \{n_1^2\Gamma_{\phi'}^2 + (n^2 - n_1^2) \sinh^2[k_0n_1\Gamma_{\phi'}(z - d)]\}^{1/2} \\ \eta(z) &= \arctan \left\{ \frac{n\gamma_{\phi'}}{n_1\Gamma_{\phi'}} \tanh[k_0n_1\Gamma_{\phi'}(z - d)] \right\}. \end{aligned} \quad (26)$$

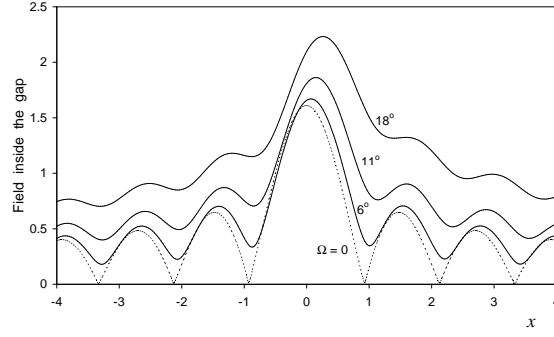


Figure 5: Total field inside the gap. The field, given by the superposition of progressive and regressive waves, was obtained by numerical integration of Eq. (26) over ϕ' , at $y = 0$ and $z = d/2$. Other parameter values are as in Fig. 3.

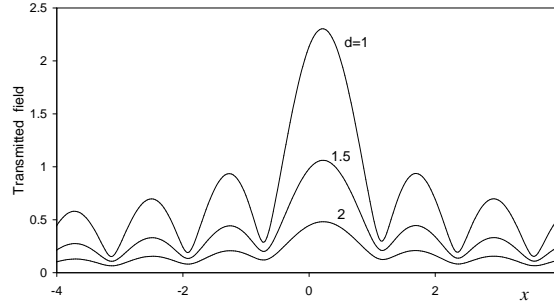


Figure 6: Transmitted field obtained by numerical integration of Eq. (18), as a function of the x coordinate, for $\Omega = 6^\circ$ and for other parameter values as in Fig. 4. With these values of the parameter, the amplitude of the field suffers a decreasing of a factor 5, by varying d from 1 to 2, while it does not suffer appreciable modification in its shape.

Again, in order to derive the total Bessel beam we have to integrate the total field (25) over ϕ' , from 0 to 2π . The amplitude of the Bessel beam inside the gap, at $z = d/2$ and $y = 0$, is shown in Fig. 5 as a function of the x coordinate, for three different values of the incidence angle Ω . We note that, for oblique incidence, the Bessel beam starts to lose its characteristic property of localized wave in the passage through the slab. In Fig. 6, we show the behavior of the transmitted field as a function of the x coordinate, for three different values of the slab's thickness. We note that the dependence on d produces a strong variation in the amplitude value, with no appreciable effect in the shape of the field: the maxima and minima positions remain unchanged. The same behavior holds also for the reflected and internal fields, with the only difference lying in the fact that the variation in the amplitude is inappreciable for the reflected field, while the amplitude is halved in the field inside the slab.

The numerical analysis was performed for an axicon angle of 60° in order to have a clearer evidence of the delocalization effect due to the passage through the slab. For smaller axicon angles, the incidence angle must also be smaller in order to have total reflection, and the effect of deformation due to oblique incidence is very poor.

An interesting aspect, related to the subject treated here, is the analysis of the wavefronts of the beam inside the slab, in order to have informations about the direction of propagation and the phase velocity in the tunneling region. This kind of analysis, however, is beyond the scope of the present work and will be reported elsewhere.

Acknowledgements

Special thanks are due to Laura Ronchi Abbozzo for useful discussions and suggestions.

References

- [1] The use of the word “beam” is accepted because the U_B field is well limited to a restricted zone of space (the first zero of J_0) along the radial coordinate.
- [2] P. Saari and K. Reivelt, Phys. Rev. Lett. **79**, 4135 (1997).
- [3] D. Mugnai, A. Ranfagni, and R. Ruggeri, Phys. Rev. Lett. **84**, 4830 (2000).
- [4] G. Toraldo di Francia, Il Nuovo Cimento **9**, 426 (1952).
- [5] J.D. Taylor ed., *Introduction to Ultra-Wideband Radar Systems* CRC, 1995.
- [6] A.M. Shaarawi and I.M. Besieris, Phys. Rev. E **62**, 7415 (2000); J. Phys. A: math. Gen. **33** (2001) 8559.
- [7] D. Mugnai, Optics Commun. **188**, 17 (2001)

- [8] A.M. Attiya, E. El-Diwany, A.M. Shaarawi, and I.M. Besieris, Progress of Electromagnetic Res., PIER **30** (2001) 191; A.M. Shaarawi, I.M. Besieris, A.M. Attiya, and E. El-Diwany, Progress of Electromagnetic Res., PIER **30** (2001) 213.
- [9] G. Toraldo di Francia, *Electromagnetic Waves*, Interscience, New York, 1955, Chap. 7.
- [10] D. Mugnai, A. Ranfagni, and L. Ronchi, Atti della Fondazione Giorgio Ronchi, **53**, 777 (1998), and arXiv:physics/0111192.
- [11] D. Mugnai, Optics Commun. **175**, 309 (2000)
- [12] However, it may be verified that the transmitted amplitude ($z > d$) propagates rigidly in the \mathbf{k}' direction (the axis of the beam) with no modification in its shape. An analogous property also holds for the reflected field.